Service Restoration for a Renewable-Powered Microgrid in Unscheduled Island Mode

Binyan Zhao, Xiaodai Dong, *Senior Member, IEEE*, and Jens Bornemann, *Fellow, IEEE*

***Abstract*—This paper deals with the service restoration problem in renewable-powered microgrids that are driven islanded by an unscheduled breakdown from the main grid. The objective is to determine the maximum of the expected restorative loads by choosing the best arrangement of the power network configurations immediately from the beginning of the breakdown all the way to the end of the island mode. The intermittency nature of the renewable power, as well as the uncertainty of the duration of the breakdown pose new challenges to this classic optimization scheduling task. The proposed two scenario-splitting methods can be solved in a two-step solving procedure, in which a Lagrangian technique and dynamic programming are utilized to provide an analytical sub-optimal yet efficient solution to the original problem. Simulation results demonstrate that both methods can find solutions very close to optima effectively; the scheduling plan should be adjusted when the time evolves, especially when the renewable power generation takes a large portion in the power supply; and the energy storage system plays a significant role to reduce the risk of unreliability in the wind power forecasting, even with a small amount of capacity. Finally, the proposed approach can be applied to radially configured systems with other types of distributed generators.**

***Index Terms*—Microgrid (MG), power network configuration, renewable power sources, service restoration (SR), unscheduled breakdown.**

NOMENCLATURE

Symbol	*Description*
$\alpha_{(.)}, \beta_{(.)}$	Priority level of critical and noncritical loads.
$\triangle_{(.,.)}$	Synchronized ramping rate of one DR unit.
ε	Convergence criterion parameter.
Δ_w	Wind power forecast error.
$\varphi_{(.,.)}, \xi_{(.,.)}, \rho^{(.)}_{(.,.)}$	Lagrangian multiplier.
μ_w	Mean of wind power forecast error.
σ_w^2	Variance of wind power forecast error.
$\Gamma(s')$	Beginning instant that scenario s does not share a bundle with scenario s'.
$\mathcal{L}^{(.)}(.)$	Lagrangian function.
$\tau^{()}$	Step size of each iteration.
$\mathfrak{T}$	Limitation of the operation times.
$c_{(.)}$	Operation cost of each switch demand can be fulfilled partially.
h (h')	State index.
i	Load point index (subscript).
j	Distributed generator index (subscript).
q	Specific bus in which the first or the second priority can be fulfilled partially.
s'	Previous scenario of scenario s.
s	Scenario index for different disconnection durations.
t	Time index (half an hour).
t_0	Initial time when the breakdown happens.
$u^*_{(.,.)}$	Optimal critical loads status indicator.
$u^{(.)}_{(.,.)}$	Critical loads status indicator where 1 means satisfied and 0 means shed.
$v^*_{(.,.)}$	Optimal noncritical loads status indicator.
$v^{(.)}_{(.,.)}$	Noncritical loads status indicator where 1 means satisfied and 0 means shed.
w_r	Wind power capacity.
$x^h_{(.,.)}$	Switch status indicator of state h where 1 means closed and 0 means open.
$\mathbf{x}_{(h,.)}$	State h consists of different status of K switches.
$C(.)$	Total cost of operation from one state to another.
cost$M$	Transfer matrix of operation cost in different states.
$D(.)$	Dual function.
DP	Dynamic programming.
DR	Distributed resource.
$E_{(.,.)}$	Critical loads in one load bus at one time instant.
$\widetilde{E}^*_{h,t}$	Actual critical loads in bus h at one time instant.
ESS	Energy storage system.
FC	Fuel cell.
$G_{(j,t)}$	Generation amounts of DR in time instant t including the target generation of wind turbines when $j = w$.
$\overline{G}_j$	Capacity of each distributed unit.
H	Total number of possible states in the power network.
$J^s_{h,t}(.)$	Return function for state h of scenario s to proceed DP.

Manuscript received July 2, 2014; revised September 22, 2014; accepted November 16, 2014. Date of publication December 12, 2014; date of current version April 17, 2015. Paper no. TSG-00673-2014.

The authors are with the Department of Electrical and Computer Engineering, University of Victoria, Victoria, BC V8W 3P6, Canada (e-mail:binyanz@ece.uvic.ca; xdong@ece.uvic.ca; jbornema@ece.uvic.ca).

Color versions of one or more of the figures in this paper are available online at http://ieeexplore.ieee.org.

Digital Object Identifier 10.1109/TSG.2014.2373272

$\overline{J}$	Probability-based expected matrix to proceed DP.
K	Total number of switches in the power network.
$L(.,.)$	Total weighted restored loads.
M	Total number of distributed units.
M_{left}	Remainder of the generation.
MT	Microturbine.
MG	Microgrid.
N	Total number of load bus.
Num$M$	Transfer matrix of operation times in different states.
$P_{s(.)}$	Probability of different cases of breakdown duration.
$\widehat{P}_{w,t}$	Forecasted wind power in time instant t.
$Q_{(.,.)}$	Noncritical loads in one load bus at one time instant.
$\widetilde{Q}^{*}_{h,t}$	Actual noncritical loads in bus h at one time instant.
S	Total number of scenarios in disconnection durations.
SR	Service restoration.
T	Total possible breakdown horizon.
TD	Time decoupled.
WPFR	Wind power forecasting reliability.
WT	Wind turbine.
$Z_{(.)}$	Restorative zone (RZ) corresponding to the distributed unit.
Z_w	RZ corresponding to the wind WT.

I. Introduction

IN RECENT years, a number of technical, cost, and societal factors came together to drive MG as one of the biggest changes in the electric power infrastructure on the horizon. Moreover, the growing penetration of renewables and other generation technologies, e.g., inverter-based small scale wind, solar photovoltaics (PV) and clean diesel, have propelled the development of MG [1]. The term MG, sometimes referred to as DR island systems, is used for some intentional islands [2]. An MG has the ability to disconnect from and parallel with the main grid so as to operate in both the "island mode" or "grid-connected." The interconnection with the main grid is being addressed via numerous pilot projects [3].

A transition-to-island mode can be triggered by a scheduled or unscheduled event [2], [4], and the latter one is the situation considered in this paper, which is an inadvertent event initiated by fault or loss of connection to the main grid. In practice, normal operations are often disrupted by sudden breakdowns and their durations are not certain but stochastic. So this situation is much more practical and challenging. In this case, the DR system needs to be automatically sectionalized through control and protection procedures, and a load management strategy is also needed in the MG blackstart operation. This can be seen as a SR problem which is a traditionally critical topic in distribution engineering [5]. The whole restoration is usually simpler for an island MG due to the reduced number of controllable variables, i.e., loads and switches. On the other hand, if there are multiple DR units in the system, the control operation should be scheduled and coordinated to efficiently fulfill the needs of the local island, while guaranteeing the system frequency and voltage requirements [6], [7] usually through a dc/ac or ac/dc/ac power electronic inverters of the DRs [8]. Besides, the whole operation requires communication and interaction among DRs and the controlling center, and the updated information should be monitored before disconnection, such as the demands, generation, and the status of the current switches at the time of breakdown, probability of each breakdown scenario, etc. Detailed MG controlling architectures and the assumed sequence of actions for MG blackstart can be referred to [8]–[11].

Considerable efforts have been placed on the analysis and methods to improve the SR plans. To achieve the restorative tasks effectively, several knowledge-based approaches have been suggested, including the expert systems [12] and artificial neural networks [13]. However, these methods only provide a reasonable numerical solution (suboptimal) and have high computational complexity. Later some optimization methods are proposed, such as branch and bound techniques combined with the interior points linear programming [14], and dynamic programming with state reduction [15]. These techniques can lead to optimal solutions but the procedure is not efficient unless large portions of the solution space can be quickly discarded when there are not too many solutions having near optimal objective values. Furthermore, most of these works consider only the deterministic SR problem, which is much simpler and saves a lot of computation and complexity. The classic PH method [16], [17] is often used to deal with general stochastic problems but it may not converge in the SR problem with uncertain breakdown time, which involves integer decision variables.

This paper deals with the SR multistage scheduling problem in an island MG system with multiple DR units consisting of a radial configuration and provides two stochastic methods to solve it. The contributions of this paper are as follows.

1) In light of the requirements of controlling procedures of MG and to take into account two types of uncertainties, i.e., the duration of disconnection and the forecasted renewable power generations, a stochastic integer problem formulation is proposed.
2) The optimization problem is solved in an efficient two-step procedure with less computation and complexity, compared to the classic PH algorithm, which is a scenario-based decomposition technique for solving stochastic programs. The comparison demonstrates the advantages of our proposed methods in terms of efficiency and accuracy.
3) The proposed methods provide guidelines to MG design, i.e., configuration of the power network, the suitable capacity of each DR unit including the ESS, to increase the reliability of the local system.

The remainder of this paper is organized as follows. Section II discusses the basic system models including demands priority, general assumptions and constraints in the island operation, as well as uncertainties in the system. Next, in Section III, the integer optimal SR problem is formulated and solved. Section IV conducts numerical simulations that verify the accuracy and feasibility of the proposed scheme. Finally, the concluding remarks are in Section V.

II. System Model

We consider the SR problem in a MG that consists of a set of M DR units, including MTs, FCs, and the WTs, and N load buses. If a general blackout occurs, local DR capabilities in an MG can be exploited to feed local customers until the main grid is reconnected. Due to the operational constraints of DRs, the local demands might not be satisfied fully but prioritized. We assume that electrical demands in the MG are prioritized into two tiers, which consists of, e.g., critical demands related to essential processes that should be met first and lower-priority noncritical demands that can be temporarily removed until adequate power is available [18]. In this paper, we use a scheduling interval of half an hour in the whole SR procedure,[1] during which demands and generations are considered constant.

A. Demands Priority

If there is insufficient generation in the MG to cover the full demands, a load-shedding scheme needs to be developed [2]. In this paper, we assume that each load bus will report the needed amount of critical loads $E_{i,t}$ and noncritical loads $Q_{i,t}$ during the breakdown horizon,[2] with α_i and β_i the priority level of the ith load bus. The total weighted loads L can be written as

$$L(u, v) = \sum_{t=t_0}^{T} \sum_{i=1}^{N} \left(\alpha_i E_{i,t} u_{i,t} + \beta_i Q_{i,t} v_{i,t}\right). \tag{1}$$

Besides, power balance within the MG island should be given careful attention [2], [20], and we divide the whole MG power network into different RZ Z_j corresponding to each DR, then we have

$$\sum_{i \in Z_j} \left(E_{i,t} u_{i,t} + Q_{i,t} v_{i,t}\right) \leq G_{j,t}. \tag{2}$$

B. General Assumptions and Islanded Operation

Under the assumption that a central control system and communication infrastructures are available for MG restoration, it is possible to produce an automatic controlling procedure after the blackout, such as identification of one or multiple suitable and stable voltage references in the MG system [8], grid synchronization [10], [11], etc. It is assumed that the information about the status of the power network, including the switch states, local demands and generations of DRs in the MG, are updated immediately after the disruption [11]. According to [8] and [10], all DR units and loads should be disconnected from the main grid at the beginning of the blackout for the stability of the system.

In order to avoid large frequency and voltage deviations, some electric utilities limit the load pick-up to 5% of the synchronized generation [2], [13], [15]. While considering the ramping rates of DRs, the constraint is expressed as

$$0 \leq G_{j,t+1} - G_{j,t} \leq \triangle_{j,t} \tag{3}$$

besides, each DR has the capacity

$$G_{j,t} \leq \overline{G}_j. \tag{4}$$

Power network reconfiguration, which is the process of altering the topology structures by changing the open/closed status $x_{k,t}$ of the sectionalizing and tie switches[3] [21], is considered as a feasible method of SR [13], [22]. However, the operational cost and the number of switching operations in the reconfiguration should be limited to achieve the restoration goal in an economical way. Then we have the total cost $C_{h,h'}$ from t to $t+1$

$$C_{h,h'} = \sum_{k=1}^{K} c_k \left| x_{k,t}^{h} - x_{k,t+1}^{h'} \right|, \; h, h' \in 1, \dots H \tag{5}$$

and the operation time constraint

$$\sum_{k=1}^{K} \left(x_{k,t} \oplus x_{k,t+1}\right) \leq \mathfrak{T} \tag{6}$$

where $\oplus$ denotes addition modulo 2. Moreover, the switch operations in the whole process should be guaranteed to restore the network into a radial structure [20], [23], which can be expressed as

$$\mathbf{x}_{h,t} \in \text{radial structure}. \tag{7}$$

C. Restorative Operation Cost and States of Network Configuration

In order to solve this restorative problem efficiently, we introduce the definition of restorative operation cost in our model, which is related to but different from [20] and [23]. In our system model are as follows.

1) Restorative operation cost is assigned to the switches needed to change status from open to closed and vice versa.
2) The operation cost c_k depends both on the distance between the load bus and the power source in the RZ Z_j and the switch type, i.e., sectionalizing or tie switches. In practice, the operation cost of each switch decreases with the reduction of the distance from the power source. It corresponds to choosing the closer de-energized area first for the restoration, in which some critical facilities are usually located. The larger cost is often assigned to the tie switches, which are of the lower operation priority in the restorative procedure. The specific operation cost strategy can be formulated by the power network designers depending on different situations.

[1]Depending on different application requirements, smaller updating intervals can be selected [19]. In practice, half an hour is meticulous for the wind power forecasting in most of the regions.

[2]We assume that the estimation of the demands on each load bus is reported accurately.

[3]There are two types of switches in distribution systems: normally closed switches which connect line sections, and normally open switches on the tie-lines which connect two primary feeders or RZ.

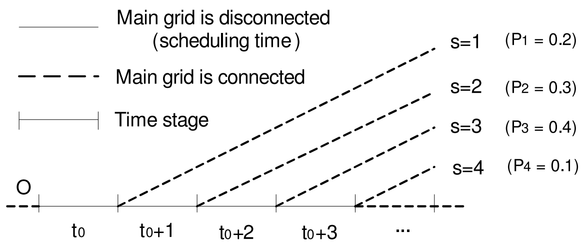

Fig. 1. Scenario tree with four scenarios, $P_s = [0.2\ 0.3\ 0.4\ 0.1]$.

3) Even in a small MG island, there are many different switch strategies, i.e., the states of network reconfiguration. However, only a small subset of them are qualified states not only conforming to the cost requirements but also the limitation of the operation times. In this paper, we denote H possible configuration states as the restorative strategies which meet the operation constraints, and then the operation cost as well as number of switch status changes can be preprocessed by $H \times H$ transfer matrices $\text{cost}M(\mathbf{x}_t, \mathbf{x}_{t+1})$ and $\text{Num}M(\mathbf{x}_t, \mathbf{x}_{t+1})$ from t to $t+1$.

D. Uncertainties in the System

1) Scenario Bundle Constraints: Scenario analysis, originally proposed by Rockafellar and Wets [16], is a widely applicable method for introducing uncertainty into practical decision problems [24]. Typically, in such problems some of the data is uncertain, and the performance measure to be optimized is the expected value of some quantity. If it is possible to delay the decision until after the uncertainty is resolved, then we are in the environment of the "wait-and-see" problem and in this case, the optimization problem is deterministic. However, often one has to make a decision without knowing in advance which scenario will occur. In such a case the optimization problem must consider all possible scenarios and choose values of the decision variables to optimize the objective function.

Here we investigate the multistage SR problem in an MG with the scenario analysis mentioned above. Although the duration of disconnecting from the main grid is uncertain, one optimal decision strategy which takes into account all the possible scenarios incorporating future time stages, must be determined and executed for the current time stage. This leads to the scenario bundle constraint. The scenarios spanning different time stages can be expressed as a scenario-tree-structure [24]–[26] in Fig. 1.

a) Scenario Tree Notation: Each leaf is connected to exactly one node at time $t \in T$, and each of these nodes represents a unique realization up to time t. Two scenarios whose leaves are both connected to the same node at time t have the same realization up to time t. Consequently, in order for a solution to be implementable it must be true that if two scenarios are connected to the same node at t, the values of the optimal variables must be the same under both scenarios for $t' \leq t$. We represent this property as a constraint by partitioning all the scenarios at each time stage into different scenario bundles.

Our restoration scheduling procedure for each scenario s begins immediately after the blackout t_0, and ends at the scheduling horizon of $T = t_0 + s - 1$. The longest possible disconnection duration is assumed to be known, i.e., the total number of scenarios S is fixed. To better present the scenario bundle constraints, we define $\Gamma(s')$ as the first period in which the scenario s does not share a bundle with the scenario s'. Then the constraints are expressed as [26], [27]

$$x_{k,t}^{s} = x_{k,t}^{s'} \tag{8}$$

$$u_{i,t}^{s} = u_{i,t}^{s'} \tag{9}$$

$$v_{i,t}^{s} = v_{i,t}^{s'},\ t = t_0, t_0+1, \ldots, \Gamma\left(s'\right) - 1. \tag{10}$$

2) WPFR: Another uncertainty comes from the nature of the fluctuating wind production over big time scale. Wind power forecasting are prone to errors, which lead to difficulties to make accurate multistage restoration schedules in MG. As in [28], we propose a similar probability based concept, WPFR, which indicates the target reliability that the wind generation forecasting can be achieved in the WTs RZ Z_w. We also assume that wind power forecast error Δ_w can be modeled as Gaussian distributed random variables [28]–[30], i.e., $\Delta_w \sim N(\mu_w, \sigma_w^2)$. Then the probabilistic power balance constraint for the wind power can be expressed as

$$P\left(\sum_{i \in Z_w} \left(E_{i,t}u_{i,t} + Q_{i,t}v_{i,t}\right) \leq \widehat{P}_{w,t} + \Delta_w\right) \geq \text{WPFR} \tag{11}$$

and is reformulated as

$$\begin{aligned}\sum_{i \in Z_w} \left(E_{i,t}u_{i,t} + Q_{i,t}v_{i,t}\right) \leq \sqrt{2}\sigma_{w,t} \times erf^{-1}(1 - 2\text{WPFR}) \\ + \widehat{P}_{w,t} + \mu_w = G_{w,t}.\end{aligned} \tag{12}$$

III. Problem Formulation and Solutions

Based upon the aforementioned system models and operational requirements in an MG, and considering the uncertainties of both wind power forecasting generation and the unforeseen breakdown from the main grid, we formulate the optimization problem as problem SR.[4] The objective is to maximize the expected restored loads while minimizing the operational cost for a horizon of multiple time instants over S possible scenarios

$$\begin{aligned}\text{SR}:\ \max_{u,v,x}\ \sum_{s=1}^{S} P_s \sum_{t=t_0}^{t_0+s-1} \Bigg(\sum_{i=1}^{N} \left(\alpha_i E_{i,t} u_{i,t}^{s} + \beta_i Q_{i,t} v_{i,t}^{s}\right) \\ - \sum_{k=1}^{K} c_k |x_{k,t}^{s} - x_{k,t+1}^{s}| \Bigg)\end{aligned}$$

s.t. (2)–(4), (6)–(10) and (12).

By observing the SR problem, we can find that in the objective function, the term $\sum_{i=1}^{N}(\alpha_i E_{i,t}u_{i,t}^{s} + \beta_i Q_{i,t}v_{i,t}^{s})$ does not contain time coupled variables, while $\sum_{k=1}^{K} c_k|x_{k,t}^{s} - x_{k,t+1}^{s}|$ does. Similar observations can be made on the constraints.

[4]Although the dimensions of $L(u, v)$ and $C(x)$ are different, the constant variables α, β, and $\mathbf{c}$ can be designed to be the weight parameters depending on different applications.

Hence we can decompose the problem into two steps. Step 1 optimizes ($\mathbf{u_t}$,$\mathbf{v_t}$) to achieve the maximum restored weighted loads by an efficient duality based subgradient method for a given network configuration, i.e., a set of $\mathbf{x_t}$, at a certain time stage. Step 2 calls DP to optimize the power network configurations, i.e., switch schemes $\mathbf{x_t}$, with the corresponding ($\mathbf{u_t}$,$\mathbf{v_t}$) from step 1 to handle the time coupled problem. To deal with the scenario parameter s and the scenario bundle constraints (8) – (10), we propose two methods. The first method puts the probability P_s into the return function of each state in every time stage of step 2, using an average return function over all relevant scenarios for each time stage. The second method treats the SR problem in a sequential manner, without considering the probability of different disconnection scenarios. Based on the optimized decision variables for the previous time stage, the optimization is carried out for the current stage.

A. Method I: Expectation Solving Procedure

We first treat problem SR as S independent sub-problems without considering the scenario bundle constraints. For each scenario s, the sub-problem is a linearly time-coupled integer problem, and a two-step solving procedure is given as follows.

Step 1: Based upon the explanation in Section II-C, we have H possible fixed network configuration states for the MG power system, and constraints (3), (4), (7) can be considered before the solving procedure. Step 1 treats the TD portion of the original SR formulation that

$$\text{TD}: \quad \max_{u,v} \sum_{i=1}^{N} \left(\alpha_i E_{i,t} u_{i,t}^s + \beta_i Q_{i,t} v_{i,t}^s\right) \quad \text{s.t. (2)} \quad (12).$$

To solve this problem analytically, we use the Lagrangian relaxation technique with Lagrangian multiplier $\rho_{j,t}$

$$\mathcal{L}_t^s\left(\rho^{\mathbf{s}}, \mathbf{u}, \mathbf{v}\right) = \sum_{i=1}^{N} -\left(\alpha_i E_{i,t} u_{i,t}^s + \beta_i Q_{i,t} v_{i,t}^s\right) + \sum_{j=1}^{M} \rho_{j,t}^s \left(\sum_{i\in Z_j} \left(E_{i,t} u_{i,t}^s + Q_{i,t} v_{i,t}^s\right) - G_{j,t}\right). \tag{13}$$

We calculate the minimization of $\mathcal{L}_t^s$ with the initial arbitrary nonnegative Lagrangian multiplier $\rho_{j,t}^s$ according to the following procedure.
The Lagrangian dual function is given by

$$D_t(\rho_{j,t}^s) = \min_{\substack{0\le u_{i,t}\le 1\\ 0\le v_{i,t}\le 1}} \mathcal{L}_t^s\left(\rho_{j,t}^s, \mathbf{u}, \mathbf{v}\right) \tag{14}$$

and the dual problem is

$$\max_{\rho_{j,t}^s\ge 0} D_t\left(\rho_{j,t}^s\right). \tag{15}$$

The dual function (14) is solved by minimizing (13) over ($\mathbf{u_t}$,$\mathbf{v_t}$). The minimum value is attained by setting $u_{i,t}^s = 1$ when the coefficient in front of $u_{i,t}^s$ is less than zero and $u_{i,t}^s = 0$ otherwise. This also applies to $v_{i,t}^s$

$$\left(u_{i,t}^s\right)^* = \begin{cases} 1 & \rho_{j,t}^s - \alpha_i < 0 \\ 0 & \text{otherwise} \end{cases} \tag{16}$$

$$\left(v_{i,t}^s\right)^* = \begin{cases} 1 & \rho_{j,t}^s - \beta_i < 0 \\ 0 & \text{otherwise.} \end{cases} \tag{17}$$

Then the subgradient method is used for solving the Lagrangian dual problem

$$\rho_{j,t}^{(n+1),s} = \left[\rho_{j,t}^{(n),s} + \tau^{(n)}\left(\sum_{i\in Z_j}\left(E_{i,t}u_{i,t}^s + Q_{i,t}v_{i,t}^s\right) - G_{j,t}\right)\right]^+. \tag{18}$$

The iterations between (16)–(18) lead to the optimal values ($\mathbf{u_t^*}$,$\mathbf{v_t^*}$) except for one element $u_{q,t}^s$ or $v_{q,t}^s$. When $\rho_{j,t}^s \ll \alpha_i$ or $\rho_{j,t}^s \gg \alpha_i$ of bus i, u_i will quickly converge to $\{0, 1\}$. This applies similarly to v_i. However, because the generation may not be exactly divided in whole to the loads on buses, there is one bus, calling it q with priority level α_q and β_q, whose load is only satisfied partially. It is observed from the iteration process that $\rho_{j,t}$ will approach to and fluctuate in the vicinity of α_q or β_q of bus q ($q \neq i$). Therefore we make the following adjustment:
when $|\rho_{j,t}^s - \alpha_q| \le \varepsilon$

$$\left(u_{q,t}^s\right)^* = 1 \tag{19}$$

$$\widetilde{E}_{q,t}^* = G_{j,t} - \sum_{i\in Z_j, i\neq q}\left(E_{i,t}\left(u_{i,t}^s\right)^* + Q_{i,t}\left(v_{i,t}^s\right)^*\right) \tag{20}$$

or when $|\rho_{j,t}^s - \beta_q| \le \varepsilon$

$$\left(v_{q,t}^s\right)^* = 1 \tag{21}$$

$$\widetilde{Q}_{q,t}^* = G_{j,t} - \sum_{i\in Z_j, i\neq q}\left(E_{i,t}\left(u_{i,t}^s\right)^* + Q_{i,t}\left(v_{i,t}^s\right)^*\right). \tag{22}$$

This means the demand on load bus q is only satisfied partially at the level of $\widetilde{E}_{q,t}^*$ or $\widetilde{Q}_{q,t}^*$. With this adjustment, all of the decision variables converge and it can be shown that problem TD is a relaxed integer linear problem, which is convex, and the duality gap between the primal problem and the dual problem is zero. A graphical convergence illustration can be found in Section IV-A.

Step 2: Given $\mathcal{D}_t(\rho_{j,t}^s)$ of every state $h \in 1, \ldots, H$ at each time stage, we will solve the time-coupled sub problem for scenario s with backward DP using Bellman function [31] given by

$$J_{h,t_0+s-1}^s = \mathcal{D}_{h,t_0+s-1}\left(\rho_{j,t_0+s-1}^s\right) + 0 \tag{23}$$

$$J_{h,t}^s = \min_{h'\in 1,\ldots,H}\left\{\mathcal{D}_{h,t}\left(\rho_{j,t}^s\right) + C_{h,h'} + J_{h',t+1}^s\right\}. \tag{24}$$

With the initial value of $J_{h,t_0+s-1}^s(\mathbf{x}_{h,t_0+s-1}^s)$ calculated from (23), for one stage t, $J_{h,t}^s(\mathbf{x}_{h,t}^s)$, i.e., the return function, is obtained by minimizing the summation of the operation cost from t to $t+1$ recorded in the transfer matrix $\text{cost}M(\mathbf{x}_t^s, \mathbf{x}_{t+1}^s)$, $\mathcal{D}_{h,t}(\rho_{j,t}^s)$ from step 1, and $J_{h',t+1}^s$, as given

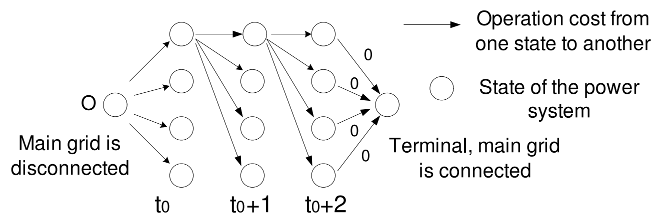

Fig. 2. DP process with time stage 3, $H = 4$. The terminal state is added with the zero operation costs.

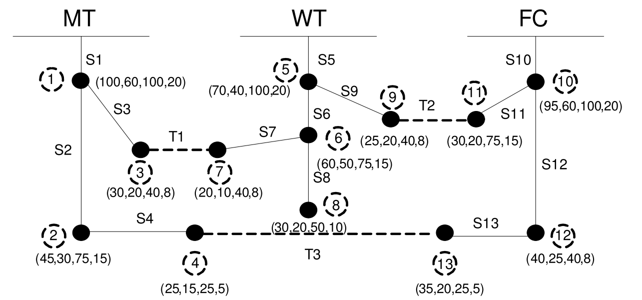

Fig. 3. System network configuration of an island MG example with coefficients of demands and priority levels ($E_{i,t}, Q_{i,t}, \alpha_{i,t}, \beta_{i,t}$).

by (24). This process continues for all the states over all time stages in scenario s. Fig. 2 illustrates the process of DP with 3 stages and 4 states.

In Method I, steps 1 and 2 are utilized to obtain the $H \times 1$ column vector J_t^s with $t = t_0, \ldots t_0 + s - 1$ at every stage t for each scenario s. To deal with the scenario bundle constraints (8)–(10), one probability-based expected matrix $\overline{J}$ with dimension $H \times S$ is created to indicate the average value of the return functions over all different scenarios. Each column of $\overline{J}$ is formulated as

$$\overline{J}_t = \sum_{s=1}^{S} P_s J_t^s \quad t = t_0, t_0 + 1, \ldots, t_0 + S - 1. \tag{25}$$

Then we find the solution h of the shortest path at the current time stage, satisfying $\min\limits_{h \in 1,\ldots,H} \{\overline{J}_t + C_{h^*,h}\}$, with h^* the network configuration solution of the previous time stage. Then the shortest path will be formed tracing forwardly from t_0 to $t_0 + S - 1$. The solution provided by Method I is sub-optimal with a small margin from the optimal results. However, the solving procedure is direct and efficient in practice.

B. Method II: Sequentially Solving Procedure

To solve Problem SR separately in different scenarios while considering the scenario bundle constraints (8)–(10), we treat the results of its previous scenario s', i.e., ($s' = s - 1$) as the reference solutions for all time stages from t_0 to $t_0 + s' - 1$ and only need to solve the problem for the current time stage t. As a result, the solving procedure is sequential and the scenario bundle constraints are satisfied at the expense of some optimality. Similar to Method I, in step 1 the analytical optimal solutions for each configuration state h at each time stage t is obtained through (14)–(22) based upon the preprocessed constraints (3), (4), and (7). As for the optimal configuration state for operation in the current time stage, we choose h' as the solution, satisfying $\min\limits_{h' \in 1,\ldots,H} \{\mathcal{D}_{h,t}(\rho_{j,t}^s) + C_{h,h'}\}$ with the previous solution h fixed as the reference. So far, we obtain the operation scheme sequentially, and note that for each scenario, only one stage optimization is needed, which is much less complex especially when the number of scenarios is large. Although the stochastic information P_s has not played a role in this method, and the operational solution is sub-optimal for the original problem SR, the solving procedure is efficient.

TABLE I
CONFIGURATIONS OF POWER NETWORK WITH $H = 11$ STATE NUMBER, AND 13 LOAD BUSES ARE DIVIDED INTO THREE RZ

SN \ *RZ*	MT	WT	FC
1	1,2,3,4	5,6,7,8,9	10,11,12,13
2	1,2,3,4	5,6,7,8,9,11	10,12,13
3	1,2,3,4	5,6,7,8	9,10,11,12,13
4	1,2,3,4,13	5,6,7,8,9	10,11,12
5	1,2,3	5,6,7,8,9	10,11,12,13
6	1,2,4	3,5,6,7,8,9	10,11,12,13
7	1,2,3,4,7	5,6,8,9	10,11,12,13
8	1,2,4	3,5,6,7,8,9,11	10,12,13
9	1,2	3,5,6,7,8,9	4,10,11,12,13
10	1,2,3,4,7	5,6,8	9,10,11,12,13
11	1,2,3,4,13	5,6,7,8,9,11	10,12

IV. SIMULATION RESULTS AND DISCUSSION

An island MG system consisting of one MT, WT, and FC, is considered for a stochastic scheduling time horizon depending on the duration of the disconnection. Our restoration strategy for the MG is further explained via an example system of Fig. 3, with the demands coefficients $E_{i,t}$, $Q_{i,t}$ kW and the priority level $\alpha_{i,t}$, $\beta_{i,t}$ of each load bus. A similar power network configuration has also been used in [22], [32], and [33]. We provide $H = 11$ candidate states for the power network configurations, i.e., different switch strategies, in Table I. The state shown in Fig. 3 is assumed to be state 1, the state immediately after the disconnection occurs. As long as the candidate configuration states are set, both of the transfer matrices cost$M_{H\times H}(x_t, x_{t+1})$ and Num$M_{H\times H}(x_t, x_{t+1})$ can be obtained. The longest possible breakdown duration is 2 h, i.e., four time instants. We assume that any generations except wind power are all zero at the moment of the disconnection occurs without loss of generality, and the assumed synchronized generations from MT and FC are $(100, 150, 250, 400)$ kW and $(100, 150, 300, 300)$ kW in four time instants, respectively. The wind speed data samples adopted in this paper are from the "Cairngorm Automatic Weather Station" in the Heriot-Watt University Physics Department [34] with the parameters $v_{\text{in}} = 3.5$ m/s, $v_r = 14$ m/s, $v_{\text{out}} = 25$ m/s, and $w_r = 400$ kW in the wind power estimation model of [28]. v_{in}, v_{out}, v_r, and w_r are cut-in, cut-out, rated wind speed, and wind power capacity for the wind power estimation, respectively.

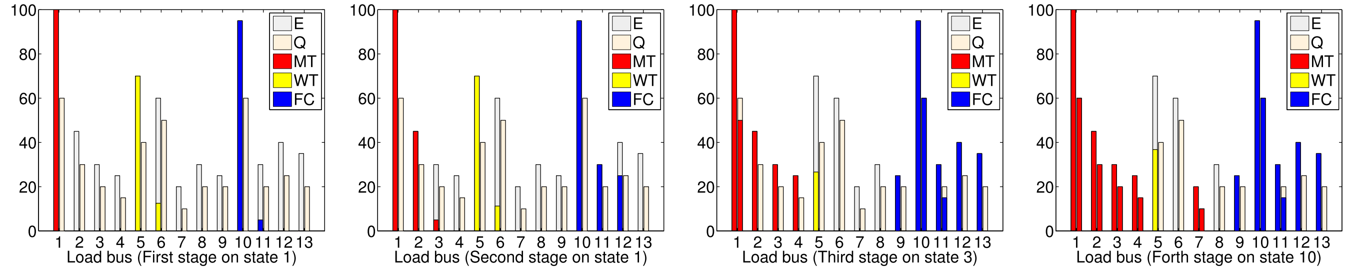

(a) (b) (c) (d)

Fig. 5. Restored loads (kW) scheduled on different load buses in four stages with shortest path states 1, 1, 3, 10.

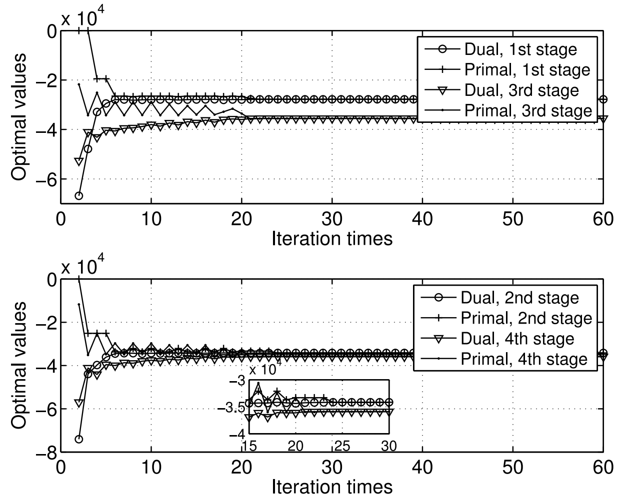

Fig. 4. Evolutions of the optimal results.

A. Restoration Schemes and Solution Convergence

This subsection illustrates the derived SR solutions mainly from the analysis of convergence and the duality gap. The probabilities of different cases P_s are set to be $[0.1, 0.4, 0.3, 0.2]$. Clearly, the longer the forecasting interval is, the less accurate the forecasted data and the bigger the variance of the forecasted error, $\sigma_{w,t}^2$. According to [28] and [29], the typical standard deviation, $\sigma_{w,t}$, of the wind power forecast error can be expressed as an approximated linear function of the forecast horizon when the forecast horizon is less than 6 hours. Thus the parameters are set as $\sigma_{w,t} = [1, 2, 3, 4]$, $\mu_w = 0$, and WPFR $= 90\%$. The evolution of the subgradient-based algorithm in Method II is illustrated in Fig. 4. All of the four stages approach convergence after about 25 iterations, which corresponds to the zero approaching duality gap. This example verifies the proposed algorithm and provides us the optimal solution effectively within each time stage. To give more insights on the restoration scheduling scheme with priorities, we provide a stage-by-stage restoration process in two tiers in Fig. 5 assuming that demands in E and Q are the same in the four stages with light colors, and different shaded areas in Fig. 5(a)–(d) illustrate different RZ from the three generators. Take Fig. 5(a) as an example. We know that in state 1, load buses 1–4 are in the same RZ supported by the generation MT. In the first stage, MT can only provide 100 kW to the bus with the highest priority α_i. It can be seen that the restored loads are increasing as the time evolves, due to the fact that the synchronized generations from MT and FC are growing.

B. Comparison of Two Scheduling Methods on Different P_s

The comparison between Methods I and II are provided in Table II. The optimal solution is obtained by the brute-force method, which is not efficient especially when the state and stage numbers are large. It can be seen that both the proposed methods are sub-optimal. The reason for this is not the process of step 1, which can provide us the optimal solution $(\mathbf{u}, \mathbf{v})$ for each time stage. The reason is due to the scenario bundle constraints resulting from the uncertainties of disconnection duration. Method II outperforms Method I when the frontal cases have greater probability of occurrence, especially in the first two cases. Since Method II is to solve the whole problem sequentially starting with scenario 1, and the following cases would follow the optimal solutions in the previous scenarios, so the result will be better if the breakdown happens more frequently with shorter durations. In contrast, Method I is an averaged result of each independent case. As for the PH method, a different initial parameter ρ leads to different results and even when we use the "variable-specific ρ" in [17], convergence is not guaranteed. The results of the proposed two methods are shown to be closer to the optima, while PH yields inferior solutions. Besides, it takes around 4 s to do the simulation with PH while the proposed methods consume 1.5 and 1.6 s, respectively, with the same parameters. The computer used is a ThinkPad Laptop with a i7 M560 duo-core processor at 2.67 GHz.

C. Adjustment of the Restoration Plan and the Effects of ESS

The uncertainties of the wind power generation will pose negative impacts on the accuracy of the restoration scheme. With the linear standard variation assumption in Section IV-A, Fig. 6 examines the alternative restoration scheduling plans on different initial points. The original scheduling plan is adjusted with the time evolution. As the initial point moves forwardly, the estimated restored loads can be more accurate due to the fact that the uncertainties of the wind power estimation is smaller. Fig. 7 illustrates the impact of ESS on dealing with the errors of wind power forecasting. We assume that a fixed amount of energy is stored in the ESS immediately after the breakdown. The ESS will be functioning in the discharging state when the real wind power of the instant is smaller than G_w, until the stored energy is used up during the breakdown, and then be in the charging function the other way round.

TABLE II
COMPARISON OF THREE SCHEDULING METHODS

Ps	Results of Different Methods					
	Method I	Method II	PH ($\rho = 100$)	PH ($\rho = 15000$)	PH (variable $\rho = c_s/(x_{max} - x_{min} + 1)$ [17])	Optimal Value
$[0.1, 0.4, 0.3, 0.2]$	83272	83505	83304	83154	83154	83683
$[0.7, 0.1, 0.1, 0.1]$	48681	48797	48684	48684	not converge	48878
$[0.1, 0.2, 0.3, 0.4]$	98043	98016	97537	97537	97537	98325
$[0.1, 0.1, 0.1, 0.7]$	113300	112800	111450	111880	111880	113300
$[0.25, 0.25, 0.25, 0.25]$	80302	80269	79986	79986	not converge	80472

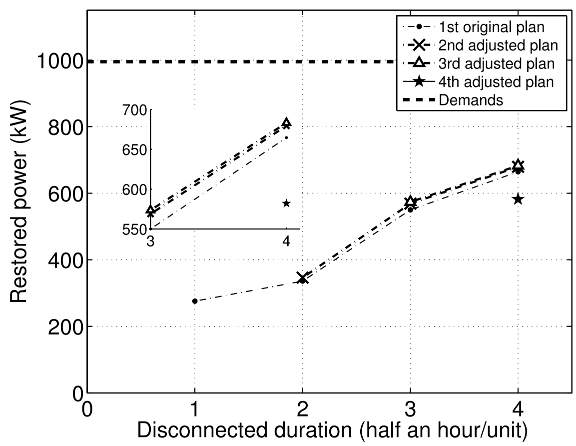

Fig. 6. Adjustments on different forecasting horizons.

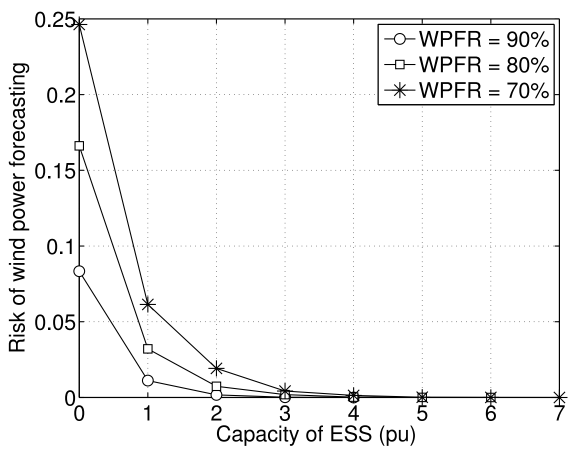

Fig. 7. Impact of ESS on the risk of unreliability of WTs, with wind power capacity = 80 p.u.

The risk of wind power forecasting is the simulated probability when the sum of the real wind power generation and the contribution of ESS is less than the target wind power generation, G_w. It can be seen from Fig. 7 that the risk caused by unreliable wind power generation decreases with the growth of the ESSs capacity, and here per-unit (p.u.) values are provided for the capacity of ESS and the wind power capacity. Although the complete characteristic of a p.u. system requires that all four base values be defined, e.g., voltage, current, power, and impedance, we consider the power scheduling and distribution here. The base power is set to be 1 p.u. = 5 kW. A huge drop of risk takes place when the wind power capacity (80 p.u.) is supported by a small capacity (1 p.u.) of ESS. This feature provides a guideline for determining the ESS size to deal with the inaccuracy of the forecasting.

V. CONCLUSION

This paper has presented two sub-optimal yet efficient solutions for SR in a MG with unscheduled disconnection from the main grid, which can be computed by a two-step procedure efficiently based upon the stochastic information. This paper illustrates that both methods can obtain solutions very close to the optimal. From the simulation results, it can be seen that the ESS plays a critical role in decreasing the negative impacts from uncertainties of the forecasted renewable power generation.

REFERENCES

[1] R. Masiello and S. Venkata, "Microgrids—There may be one in your future," *IEEE Power Energy Mag.*, vol. 11, no. 4, pp. 14–93, Jun. 2013.

[2] *IEEE Guide for Design, Operation, and Integration of Distributed Resource Island Systems With Electric Power Systems*, IEEE Standard 1547.4, Jul. 2011.

[3] *Smart Grid Research and Development Multi-Year Program Plan (2010-2014)*, U.S. Dept. Energy, Washington, DC, USA, Tech. Rep., Sep. 2012. [Online]. Available: http://energy.gov/oe/downloads/smart-grid-rd-multi-yearprogram-plan-2010-2014-september-2012-update

[4] H. Laaksonen and K. Kauhaniemi, "Control principles for black start and island operation of microgrid," in *Proc. Nordic Workshop Power Ind. Electron.*, Jun. 2008, pp. 1–8.

[5] L. Fink, K. Liou, and C. Liu, "From generic restoration actions to specific restoration strategies," *IEEE Trans. Power Syst.*, vol. 10, no. 2, pp. 745–752, May 1995.

[6] *American National Standard for Electric Power Systems and Equipment Voltage Ratings (60 Hertz)*, ANSI standard C84.1, 2011.

[7] *IEEE Draft Standard for Interconnecting Distributed Resources With Electric Power Systems*, IEEE WG Standard 1547-2003, Jul. 2001.

[8] J. A. Lopes, C. L. Moreira, and A. G. Madureira, "Defining control strategies for microgrids islanded operation," *IEEE Trans. Power Syst.*, vol. 21, no. 2, pp. 916–924, May 2006.

[9] Y. Mao and K. Miu, "Switch placement to improve system reliability for radial distribution systems with distributed generation," *IEEE Trans. Power Syst.*, vol. 18, no. 4, pp. 1346–1352, Nov. 2003.

[10] S. Thale and V. Agarwal, "A smart control strategy for the black start of a microgrid based on PV and other auxiliary sources under islanded condition," in *Proc. IEEE Photovol. Spec. Conf.*, Seattle, WA, USA, 2011, pp. 2454–2459.

[11] C. Moreira, F. Resende, and J. Lopes, "Using low voltage microgrids for service restoration," *IEEE Trans. Power Syst.*, vol. 22, no. 1, pp. 395–403, Feb. 2007.

[12] Y. Fukuyama and H. Endo, "A hybrid system for service restoration using expert system and genetic algorithm," in *Proc. IEEE Int. Conf. Intell. Syst. Appl. Power Syst.*, Orlando, FL, USA, 1996, pp. 394–398.

[13] Y. Hsu and H. Huang, "Distribution system service restoration using the artificial neural network approach and pattern recognition method," *IEEE Proc. Gener. Transmiss. Distrib.*, vol. 142, no. 3, pp. 251–256, May 1995.

[14] J. Momoh and A. Caven, "Distribution system reconfiguration scheme using integer interior point programming technique," in *Proc. IEEE PES Transmiss. Distrib. Conf. Expo.*, vol. 1. Dallas, TX, USA, 2003, pp. 234–241.

[15] R. Pérez-Guerrero, G. T. Heydt, N. J. Jack, B. K. Keel, and A. R. C. Castelhano, "Optimal restoration of distribution systems using dynamic programming," *IEEE Trans. Power Del.*, vol. 23, no. 3, pp. 1589–1596, Jul. 2008.

[16] R. Rockafellar and R. Wets, "Scenarios and policy aggregation in optimization under uncertainty," *Math. Oper. Res.*, vol. 16, no. 1, pp. 119–147, 2008.

[17] J. P. Watson, D. L. Woodruff, and D. R. Strip, "Progressive hedging innovations for a class of stochastic resource allocation problems," *Comput. Manage. Sci.*, vol. 8, no. 4, pp. 355–370, 1997.

[18] M. Pipattanasomporn, H. Feroze, and S. Rahman, "Multi-agent systems in a distributed smart grid: Design and implementation," in *Proc. IEEE/PES Power Syst. Conf. Expo.*, Seattle, WA, USA, Mar. 2009, pp. 1–8.

[19] M. Klemen, "Wind speed data and its application to wind generated power," *Homepower*, vol. 62, no. 2, pp. 34–38, 1997.

[20] T. Nagata and H. Sasaki, "An efficient algorithm for distribution network restoration," in *Proc. Power Eng. Soc. Summer Meeting*, Vancouver, BC, Canada, 2001, pp. 54–59.

[21] H. Chiang and R. Jumeau, "Optimal network reconfigurations in distribution systems II: Solution algorithms and numerical results," *IEEE Trans. Power Del.*, vol. 5, no. 3, pp. 1568–1574, Jul. 1990.

[22] C. Su and C. Lee, "Network reconfiguration of distribution systems using improved mixed-integer hybrid differential evolution," *IEEE Trans. Power Del.*, vol. 18, no. 3, pp. 1022–1027, Jul. 2003.

[23] A. Zidan and E. El-Saadany, "A cooperative multiagent framework for self-healing mechanisms in distribution systems," *IEEE Trans. Smart Grid*, vol. 3, no. 3, pp. 1525–1539, Sep. 2012.

[24] J. Mulvey and A. Ruszczynski, "A new scenario decomposition method for large-scale stochastic optimization," *Oper. Res.*, vol. 43, no. 3, pp. 477–490, 1995.

[25] Z. Chen, S. Li, and D. Tirupati, "A scenario-based stochastic programming approach for technology and capacity planning," *Comput. Oper. Res.*, vol. 29, no. 7, pp. 781–806, Jun. 2002.

[26] L. Tang, P. Che, and J. Wang, "Corrective unit commitment to an unforeseen unit breakdown," *IEEE Trans. Power Syst.*, vol. 27, no. 4, pp. 1729–1740, Nov. 2012.

[27] S. Takriti and J. Birge, "Lagrangian solution techniques and bounds for loosely coupled mixed-integer stochastic programs," *Oper. Res.*, vol. 48, no. 1, pp. 91–98, 2000.

[28] B. Zhao, Y. Shi, X. Dong, W. Luan, and J. Bornemann, "Short-term operation scheduling in renewable-powered microgrids: A duality-based approach," *IEEE Trans. Sustain. Energy*, vol. 5, no. 1, pp. 209–217, Jan. 2014.

[29] R. Doherty and M. O'Malley, "A new approach to quantify reserve demand in systems with significant installed wind capacity," *IEEE Trans. Power Syst.*, vol. 20, no. 2, pp. 587–595, May 2005.

[30] S. Tewari, C. J. Geyer, and N. Mohan, "A statistical model for wind power forecast error and its application to the estimation of penalties in liberalized markets," *IEEE Trans. Power Syst.*, vol. 26, no. 4, pp. 2031–2039, Nov. 2011.

[31] J. Muckstadt and S. Koenig, "An application of Lagrangian relaxation to scheduling in power-generation systems," *Oper. Res.*, vol. 25, no. 3, pp. 387–403, 1977.

[32] S. Civanlar, J. Grainger, H. Yin, and S. Lee, "Distribution feeder reconfiguration for loss reduction," *IEEE Trans. Power Del.*, vol. 3, no. 3, pp. 1217–1223, Jul. 1988.

[33] T. Ou, W. Lin, C. Huang, and F. Cheng, "A hybrid programming for distribution reconfiguration of dc microgrid," in *Proc. IEEE PES Conf. Sustain. Altern. Energy*, Valencia, Spain, 2009, pp. 1–7.

[34] (Dec. 3, 2014). *Cairngorm Automatic Weather Station*. [Online]. Available: http://cairngormweather.eps.hw.ac.uk/archive.htm

Binyan Zhao received the B.Sc. and M.Sc. degree in telecommunication from the Beijing University of Posts and Telecommunications, Beijing, China, in 2008 and 2011, respectively. She is currently pursuing the Ph.D. degree in electrical and computer engineering at the University of Victoria, Victoria, BC, Canada.

Her current research interests include scheduling problems in distribution power network and service restoration issues in microgrid. In 2014, she was with Alpha Technology, Ltd., Burnaby, BC, Canada, for an eight month internship.

Xiaodai Dong (S'97–M'00–SM'09) received the B.Sc. degree in information and control engineering from Xi'an Jiaotong University, Xi'an, China; the M.Sc. degree in electrical engineering from the National University of Singapore, Singapore; and the Ph.D. degree in electrical and computer engineering from Queen's University, Kingston, ON, Canada, in 1992, 1995, and 2000, respectively.

From 1999 to 2002, she was with Nortel Networks, Ottawa, ON, and served on the base transceiver design of the third-generation (3G) mobile communication systems. From 2002 to 2004, she was an Assistant Professor with the Department of Electrical and Computer Engineering, University of Alberta, Edmonton, AB, Canada. Since 2005, she has been with the University of Victoria, Victoria, BC, Canada, where she is currently a Professor and a Canada Research Chair (Tier II) in the Department of Electrical and Computer Engineering.

Jens Bornemann (M'87–SM'90–F'02) received the Dipl.-Ing. and the Dr.-Ing. degrees in electrical engineering from the University of Bremen, Bremen, Germany, in 1980 and 1984, respectively.

From 1984 to 1985, he worked as a private engineering consultant. In 1985, he joined the University of Bremen as an Assistant Professor. Since 1988, he has been with the Department of Electrical and Computer Engineering, University of Victoria, Victoria, BC, Canada, where he became a Professor in 1992. From 1992 to 1995, he was a Fellow of the British Columbia Advanced Systems Institute, Vancouver, BC, Canada. In 1996, he was a Visiting Scientist with Spar Aerospace, Ltd., (currently MDA Space), Québec City, QC, Canada, and a Visiting Professor with the Microwave Department, University of Ulm, Ulm, Germany. In 2003, he was a Visiting Professor with the Laboratory for Electromagnetic Fields and Microwave Electronics, ETH Zurich, Zurich, Switzerland. From 1997 to 2002, he was a Co-Director at the Center for Advanced Materials and Related Technology, University of Victoria. He is a Registered Professional Engineer with the Province of British Columbia, Canada. His current research interests include radio frequency/wireless/microwave/millimeter-wave components and systems design, field-theory-based modeling of integrated circuits, feed networks, and ultrawideband technology and antennas. He has co-authored the book *Waveguide Components for Antenna Feed Systems—Theory and Design* (Artech House, 1993) and has authored/co-authored over 300 technical papers.

Dr. Bornemann served as an Associate Editor of the IEEE TRANSACTIONS ON MICROWAVE THEORY AND TECHNIQUES in the areas of microwave modeling and computer-aided design from 1999 to 2002, and the *International Journal of Electronics and Communications* from 2006 to 2008. From 1999 to 2009, he served on the Technical Program Committee of the IEEE Microwave Theory and Techniques Society International Microwave Symposium. He serves on the Editorial Advisory Board of the *International Journal of Numerical Modeling*. He is a Fellow of the Canadian Academy of Engineering.